

Successful strategies in size structured mixotrophic food webs

Selina Våge · Marco Castellani · Jarl Giske ·
T. Frede Thingstad

Received: 21 January 2013 / Accepted: 17 July 2013 / Published online: 31 July 2013
© Springer Science+Business Media Dordrecht 2013

Abstract This study investigates how food web structures in aquatic microbial communities emerge based on different mixotrophic life strategies. Unicellular mixotrophic organisms that combine osmotrophy and primary production with phagotrophy account for significant amounts of primary production and bacterivory in marine environments, yet mixotrophs are still usually absent in large-scale biogeochemical models. We here present for the first time a thorough analysis of a food web model with a finely resolved structure in both cell size and foraging mode, where foraging mode is a strategy ranging from pure osmotrophy to pure phagotrophy. A trade-off for maximum uptake rates of mixotrophs is incorporated. We study how different factors determine the food web structure, here represented by the topology of the distribution of given amounts of total phosphorous over the cell size-foraging mode plane. We find that mixotrophs successfully coexist with foraging specialists (pure osmo- and phagotrophs) for a wide range of conditions, a result consistent with the observed prevalence

of mixotrophs in recent oceanographic surveys. Mixotrophy trade-off and size-dependent parameters have a strong effect on the emerging community structure, stressing the importance of foraging mode and size considerations when working with microbial diversity and food web dynamics. The proposed model may be used to develop timely representations of mixotrophic strategies in larger biogeochemical ocean models.

Keywords High-resolution planktonic food web model · Coexistence · Mixotrophic diversity · Cell size · Foraging mode

Introduction

Mixotrophy encompasses diverse foraging strategies in unicellular organisms, which combine auto- and heterotrophic nutrition. Mixotrophs are ecologically more important than traditionally assumed (Unrein et al. 2007; Hartmann et al. 2012). In the pelagic environment, mixotrophy often occurs in oligotrophic and non-equilibrium environments, but it is also a major nutritional mode in eutrophic waters during harmful algal blooms (Burkholder et al. 2008; Sanders 2011). Around 50 % of the pigmented biomass and up to 90 % of bacterivory can be accounted for by mixotrophs in coastal areas and central gyres of the North Atlantic (Havskum and Riemann 1996; Zubkov and Tarran 2008). Mixotrophs can increase the system productivity and stability (Baretta-Bekker et al. 1998;

Handling Editor: Piet Spaak.

Electronic supplementary material The online version of this article (doi:10.1007/s10452-013-9447-y) contains supplementary material, which is available to authorized users.

S. Våge (✉) · M. Castellani · J. Giske · T. F. Thingstad
Department of Biology, University of Bergen,
5020 Bergen, Norway
e-mail: selina.vage@bio.uib.no

Hammer and Pitchford 2005) and affect biogeochemical cycling of nutrients by using varying degrees of phototrophic and heterotrophic activities (Mitra and Flynn 2010). It is therefore an important task for aquatic ecologists to understand the prevailing success of mixotrophs.

Mixotrophs compete with pure auto- and heterotrophs (referred to as specialists below) for resources. It is not immediately obvious how mixotrophs can coexist or in some cases even dominate over foraging specialists. Maintaining two different nutritional systems is expected to be expensive as it may induce space conflicts for external resource uptake sites on the cell surface (Flynn and Mitra 2009; Ward et al. 2011). Pure auto- and heterotrophs are thus often considered to be competitively superior to mixotrophs in non-limiting environments. Some experiments support this idea (Rothhaupt 1996), while others challenge it (McKie-Kriesberg et al. 2011). Still, the actual costs and trade-offs of mixotrophy remain hypothetical, and there is insufficient evidence to confirm that mixotrophs are competitively inferior to specialists (Stoecker 1998; Litchman et al. 2007).

Mixotrophy is often neglected in large-scale ecosystem models, despite the frequent occurrence of this strategy in nature, its significant role in harmful algal blooms and its potential impact on elemental cycling. Theoretical studies working on mixotrophy have typically focused on the effect of mixotrophs on the planktonic ecosystem dynamics by incorporating one mixotrophic functional group into Lotka–Volterra type models (Thingstad et al. 1996; Stickney et al. 2000). In such models, mixotrophs represent additional and important pathways for organic matter transfer in the food web. They also appear to have a stabilizing effect on the system dynamics (Jost et al. 2004). Some models including one functional mixotrophic group were used to study coexistence of mixotrophs and specialists. In these models, mixotrophs with a strong degree of autotrophy are typically most successful (Thingstad et al. 1996; Crane and Grover 2010).

While models including a single mixotrophic functional type give general insights on food web dynamics, mixotrophic foraging strategies are highly diverse in nature, ranging from nearly pure auto- to almost pure heterotrophy (Stoecker 1998). The question how several different mixotrophic strategies can coexist has rarely been addressed so far. Exceptions

include Troost et al. (2005), who studied the conditions when specialists evolve from mixotrophs by using affinities for the autotrophic and heterotrophic pathway as evolutionary parameters. Cell size was not included as a variable trait in their model. Also, Ward et al. (2011) showed that a range of different mixotrophic strategies can persist over time when uptake rates are diffusion limited (i.e. in oligotrophic environments). They predict that large mixotrophs succeed when the limiting process changes from diffusion to cross-membrane transport, whereas smaller mixotrophs are restricted to oligotrophic regions. Neither they did include organism size as a model parameter to actually test this hypothesis.

Organism size is an important ecological trait that strongly influences both ecosystem structure and individual processes such as metabolic rates and trophic interactions (Loeuille et al. 2005; Thingstad et al. 2005b). The pelagic microbial food web is particularly interesting for studying effects of organism size, as it covers several orders of magnitude of cell size. Mixotrophic members range from small nanoflagellates (2–20 μm diameter) to large dinoflagellates and ciliates (some 100 μm diameters).

Furthermore, size-selective feeding is known to have a strong effect on the structure of the pelagic food web (Thingstad et al. 2005b). A review by Hansen et al. (1994) highlights varying optimal prey sizes for different predators, resulting in optimal predator to prey size ratios (SRs) ranging from 1:1 for dinoflagellates (i.e. the prey's estimated spherical diameter is equal to the predator's) to 50:1 for cladocerans and meroplankton larvae (where the predator's estimated spherical diameter is 50 times larger than the prey's). Nanoflagellates and ciliates have optimal SR of around 3:1 and 8:1, respectively. Even though optimal SR and different size classes affect food web structures and dynamics, they often remain insufficiently resolved in contemporary ecological models. An exception is Moloney and Field (1991), who resolved size classes in their model to study size-based dynamics of plankton food webs.

Despite the significance of cell size, SR and foraging mode on food web structures, none of the previous modeling studies have combined several size classes with different foraging modes, although varying cell sizes and degrees of mixotrophy can influence biogeochemical processes and community structures in different ways (Loeuille et al. 2005; Thingstad

et al. 2005b; Stoecker 1998). For example, small nanoflagellates eating bacteria may increase the flux from the microbial loop to higher trophic levels, whereas the larger dinoflagellates eating large ciliates could have the opposite effect (Stoecker 1998). In light of the recently recognized importance of mixotrophy in the pelagic environment and the well-known importance of cell size on system processes and cell physiologies, it is timely to resolve and study both traits in a single model.

To improve our understanding of the ecological mechanisms that shape food web structures and maintain a high diversity of different foraging modes and organism sizes in the pelagic ecosystem, we developed a highly resolved differential equation-based model of a pelagic microbial food web, where a large number of organisms with different foraging modes and cell sizes interact. The system is mineral nutrient limited, where foraging modes range between osmotrophy (uptake of dissolved inorganic nutrients) and phagotrophy (uptake of nutrients as prey particles). Following Castellani et al. (2012), mixotrophy is modeled using a trade-off parameter τ for maximum resource uptake rates, which reduces competitive abilities of mixotrophs relative to specialists when τ is larger than 1. We do not consider light and its effects on mixotrophy in carbon limited systems.

We hypothesize that the success of different cell sizes and foraging modes depends on particular conditions. By varying several parameters such as the total nutrient content in the system, the optimal SR, the foraging trade-off, and the size dependency of resource uptake rates, the model indicates when particular strategies may be successful in nature. We show that mixotrophic organisms of varying sizes successfully coexist with, and occasionally outcompete, foraging specialists for a range of different parameter values and that size-depending parameters as well as the foraging mode trade-off have a strong influence on the emerging food web structure.

Model

The study is conducted using a differential equation-based model of a microbial food web that is structured by cell size and foraging mode. Cell sizes are divided into 32 classes ranging from 0.5 to 643 μm cell diameters. Hence, organisms from the size of small

bacteria to large protozoans are covered. Also, following the concept of a mixotrophic gradient (Sanders et al. 1990), 11 foraging modes (f) ranging from pure osmotrophy ($f = 0$) to pure phagotrophy ($f = 1$) are simulated for each size class. This gives a food web consisting of 32×11 compartments. The matrix formed by these 32×11 compartments is referred to as ‘cell size–foraging mode plane’ below.

Cell masses double between each size class, giving a logarithmic cell size distribution in the simulated food web. The organisms’ biomasses are given in units of phosphorous and are based on their volumes, assuming spherical cells and equal stoichiometry for all organisms. Thereby derived cell mass proxies range from 1.6×10^{-8} nmol-P for the smallest organisms (with a cell diameter of 0.5 μm) to about 33 nmol-P for the largest organisms (with a cell diameter of roughly 643 μm). The system is closed and the total amount of phosphorous set to 500 nmol-P L^{-1} per default. Nutrients are released during grazing or death and are immediately recirculated to the shared dissolved inorganic phosphorous (DIP) pool. Differential equations describe the mass budgets for each of the 32×11 compartments based on the gains from osmotrophic and phagotrophic feeding activities and the losses due to predation and other losses such as metabolism (Eq. 1). The differential equations and model parameters are given in Table 1, whereas the symbols and default parameter values used in this study are given in Table 2. A justification of the parameter values is given in the sections “Simulations” and “Discussion”.

The uptake rate for dissolved phosphorous is described by the maximum uptake rate for DIP ($v_{\text{max}}\text{DIP}$) and the nutrient affinity α (Eq. 1a), while the uptake rate of prey is described by the maximum prey uptake rate ($v_{\text{max}}\text{prey}$) and the clearance rate β (Eq. 1b). The nutrient affinity α and the clearance rate β describe the slope of the uptake rate function at the origin for DIP and prey, respectively, where resource encounters are diffusion limited (Fig. 1a).

Maximum cell-specific uptake rates are proportional to the cell surface (Aksnes and Cao 2011). To obtain a biomass-specific maximum uptake rate, the cell-specific rate is divided by the cell mass, which scales with the cell volume. Hence, the biomass-specific maximum uptake rates for DIP (Eq. 2) and prey (Eq. 3) decrease linearly with increasing cell diameter ($V_{\text{max}} \propto \text{diam}^{-1}$). Furthermore, the maximum

Table 1 Differential equations (1) and maximum phosphorous uptake rates for DIP (2) and prey (3), as well as cell mass specific nutrient affinities (4) and effective clearance rates (5) for model compartments ij

Equation	Number
Differential equation for compartment ij :	
$\frac{dM}{dt}_{ij} = \text{OsmoGain}_{ij} + \text{PhagoGain}_{ij} - \text{LossAsPrey}_{ij} - \text{OtherLoss}_{ij}$	(1)
$\text{OsmoGain}_{ij} = \frac{\alpha_i * \text{DIP}}{1 + \frac{\text{DIP}}{V_{\max} \text{DIP}_{ij}}} * M_{ij}$ (DIP uptake)	(1a)
$\text{PhagoGain}_{ij} = \sum_{\text{prey}} \left(\frac{\beta_{i,\text{prey}} * M_{\text{prey}}}{1 + \frac{\beta_{i,\text{prey}} * M_{\text{prey}}}{V_{\max} \text{prey}_{ij}}} \right) * \text{yield} * M_{ij}$ (prey uptake)	(1b)
$\text{LossAsPrey}_{ij} = \sum_{\text{pred}} \left(\frac{\beta_{\text{pred},i} * M_{ij}}{1 + \frac{\beta_{\text{pred},i} * M_{ij}}{V_{\max} \text{prey}_{\text{pred}}}} * M_{\text{pred}} \right)$ (predation loss)	(1c)
$\text{OtherLoss}_{ij} = \delta * M_{ij}$	(1d)
Maximum phosphorous uptake rates for DIP (cell size i and foraging mode j dependent):	
$V_{\max} \text{DIP}_{ij} = V_{\max} \text{DIP}_0 * \left(\frac{\text{diam}_i}{\text{diam}_0} \right)^{-\tau} * (1 - f_j)^\tau$	(2)
Maximum phosphorous uptake rate for prey (cell size i and foraging mode j dependent):	
$V_{\max} \text{prey}_{ij} = V_{\max} \text{prey}_0 * \left(\frac{\text{diam}_i}{\text{diam}_{\text{phag0}}} \right)^{-\tau} * (f_j)^\tau$	(3)
Mineral nutrient (DIP) affinity (cell size dependent):	
$\alpha_i = \alpha_0 * \left(\frac{\text{diam}_i}{\text{diam}_0} \right)^{-x}$	(4)
Clearance rate on prey p (cell size i and prey size prey dependent, normally distributed around prey with optimal predator to prey size ratio):	
$\beta_{i,\text{prey}} = \beta_0 * e^{-\left(\frac{SC_i - SC_{\text{prey}} - P2P}{SW} \right)^2} * \left(\frac{\text{diam}_i}{\text{diam}_{\text{phag0}}} \right)^{-x}$	(5)

Size and foraging mode classes are indexed with i and j , respectively. In Eqs. 1b and 1c, the summations with indices prey and pred loop through all 32×11 compartments, covering all potential prey and predators of compartment ij

uptake rate for DIP increases with increasing osmotrophy (f approaching 0), while the maximum uptake rate for prey increases with increasing phagotrophy (f approaching 1). A trade-off parameter $\tau > 0$ is incorporated in Eqs. 2 and 3, which accounts for an assumed trade-off in maximum uptake rates for mixotrophic foraging strategies relative to specialized foraging. For a high trade-off parameter ($\tau > 1$), the maximum phosphorous uptake rate initially decreases rapidly for increasing f , whereas the maximum prey uptake rate only increases slowly compared to the specialist's uptake rates (Fig. 1b, $\tau = 4$). This represents a high cost of mixotrophy since a modest gain in terms of increased maximum prey uptake rate is accompanied by a drastic loss of the maximum DIP uptake rate ('gain is less than loss'). For a low trade-off parameter ($\tau < 1$), on the other hand, $V_{\max} \text{prey}$ initially increases rapidly for increasing f , whereas $V_{\max} \text{DIP}$ decreases only slowly. This has the effect that highly increased phagotrophic ability only slightly reduces the osmotrophic ability of the mixotroph ('gain is more than loss') (Fig. 1b, $\tau = 0.5$). For $\tau = 1$, the reduction in uptake rate for one resource is proportional to the

gain in the uptake rate for the other resource, and vice versa (Fig. 1b, straight lines).

Whereas maximum uptake rates in our model are assumed to be influenced by biological constraints, and therefore vary depending on the foraging mode and trade-off (Fig. 2, lower left), the nutrient affinities and clearance rates describing the slope of the uptake function at the origin are assumed to be purely diffusion limited. They are determined by physical constraints of molecular diffusion at low resource concentrations. Assuming that the cell concentration of the limiting nutrient is independent of the cell volume, this leads to a decrease of α and β with the square of the diameter ($\alpha, \beta \propto \text{diam}^{-2}$, Fig. 2, upper right) (e.g. Tambi et al. 2009).

In our model, interactions between organisms happen through predation across size classes and competition for DIP (Eq. 5). Prey are selected according to their size, with the clearance rate being normally distributed around the prey with the optimal SR (Eq. 5, Fig. 2, lower right). We name the standard deviation of this normally distributed clearance rate the 'prey spectrum width' (SW), which is set to 1 size

Table 2 Symbols and parameter values used in the default setting

Name	Value	Units	Description
diam ₀	0.5	μm	Diameter of smallest organism
mass ₀	1.6 × 10 ⁻⁸	nmol-P	Mass of smallest organism
mass _{phag0}	mass ₀ *2 ^{P2P}	nmol-P	Mass of smallest phagotroph
diam _{phag0}	diam ₀ *(2 ^{P2P}) ^{1/3}	μm	Diameter of smallest phagotroph
diam _i		μm	Diameter of size class <i>i</i>
f _j	0 ≤ f ≤ 1		Foraging mode (0: pure osmo-, 1: pure phagotrophy)
α ₀	0.4	L h ⁻¹ nmol-P ⁻¹	Nutrient affinity of smallest osmotroph
β ₀	0.001	L h ⁻¹ nmol-P ⁻¹	Clearance rate of smallest phagotroph
V _{max} DIP ₀	1/6	h ⁻¹	Max. DIP uptake for smallest osmotroph
V _{max} prey ₀	200*2 ^{-P2P}	h ⁻¹	Max. prey uptake for smallest phagotroph
δ	0.001	h ⁻¹	Metabolic loss or non-predatory mortality
M _{ij}	0 ≤ M _{ij} ≤ 500	nmol-P L ⁻¹	Total mass in compartment <i>ij</i> (<i>i</i> size class; <i>j</i> foraging mode)
τ	0.5, 4		Mixotrophy trade-off
yield	0.3		Yield from phagotrophic uptake
x	2		Exponential factor by which α and β decrease as the cell diameter increases
y	1		Exponential factor by which V _{max} prey and V _{max} DIP decrease with increasing diameter
P2P	7, 10		Predator to prey size class ratio (# of size classes)
SR	5, 10		Predator to prey diameter ratio (SR = (2 ^{P2P}) ^{1/3})
SW	1, 2, 4		Prey spectrum width (# of size classes)
SC	1–32		Size class index
P _{tot}	500	nmol-P L ⁻¹	Total phosphorous in the system
DIP _{initial}	0.001*P _{tot}	nmol-P L ⁻¹	Initial DIP concentration

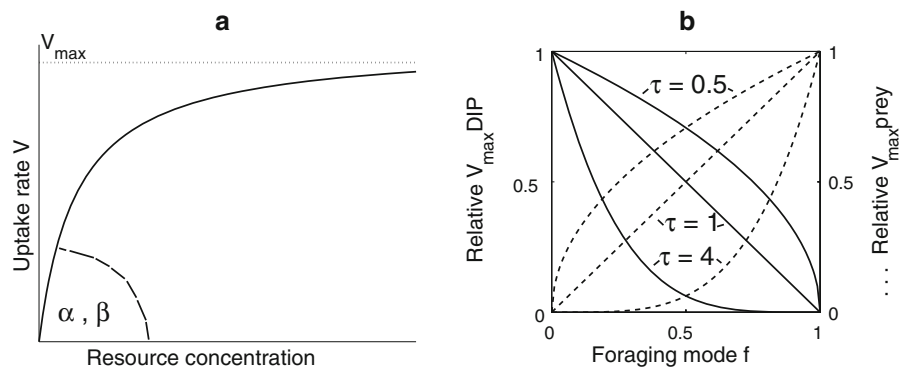


Fig. 1 **a** Schematic Holling type II functional response. The nutrient affinity α (in osmotrophy, Eq. 1a) and the clearance rate β (in phagotrophy, Eq. 1b) represent the angle of the uptake rate at the origin and accurately describe the rate at low resource concentrations. At high resource concentrations, the uptake rate asymptotically approaches the maximum uptake rates (V_{max} in Eqs. 1a and 1b). **b** Relative maximum DIP (solid lines, Eq. 2) and

prey uptake rates (dotted lines, Eq. 3) as functions of the foraging mode f and trade-off τ ($f = 0$ is pure osmo-, $f = 1$ pure phagotrophy). Curves are shown for a low ($\tau = 0.5$) and high trade-off ($\tau = 4$), which are values mostly used in this study. Straight lines for $\tau = 1$ are included as reference. For an explanation of the trade-off curves, see text

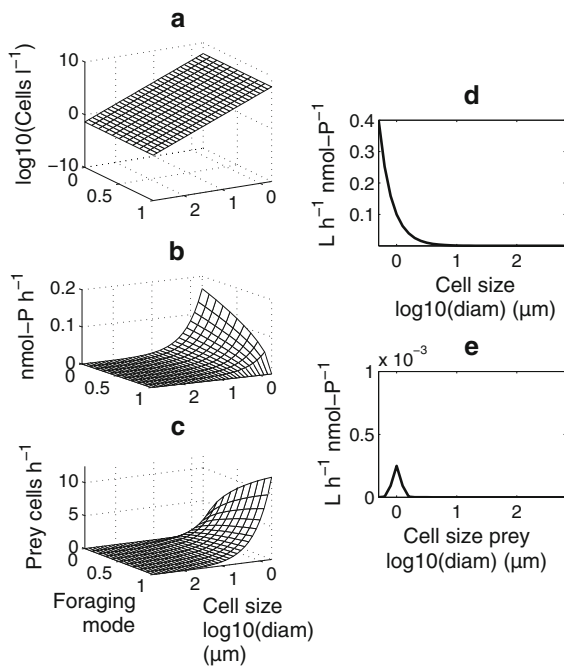


Fig. 2 Initial abundance (a) and cell mass specific maximum DIP (b) and prey uptake rates (c) as functions of cell size and foraging mode, as well as cell mass specific nutrient affinity (d) and clearance rate (e) as functions of cell size. Note that the clearance rate on prey of all sizes is shown for a predator of the 10th size class. The clearance rate on a particular prey class decreases for predators with increasing size, analogously to the nutrient affinity (d)

class per default. The optimal SR in terms of diameters is varied between 1 (i.e. the prey's estimated spherical diameter equals the predator's) and 10 (where the predator's estimated spherical diameter is 10 times larger than the prey's). Imitating a natural state of planktonic systems (Sheldon et al. 1972), the system is initialized with a uniform mass distribution in all size classes and foraging mode compartments, leading to a highest abundance of the smallest organisms (Fig. 2, upper left).

The model was implemented and the simulations run using Matlab Version R20011a. Equation 1 was integrated using the Matlab ODE23 implementation of the explicit Bogacki and Shampine third-order Runge–Kutta method (Shampine and Reichelt 1997). An individual-based version of the model was developed by Castellani et al. (2012), who presented a new method to address issues related to individual-based modeling of largely in-homogenous population densities, as in the case of pelagic microbial food webs.

Simulations

The system of differential equations was simulated for 10 years for each set of tested parameters. This was sufficient for the established populations (defining the occupied space in the cell size–foraging mode plane) to stabilize in terms of abundance. The 10th year's mean mass distribution in the cell size–foraging mode plane was plotted. The default parameter values used in the simulations are given in Table 2. Sensitivity to the parameters was tested by varying selected parameters as described below, illustrating the effect of different factors on the food web structure.

Variations of parameters

Foraging mode and cell size were investigated as response variables to changes of the parameters described in the following paragraphs. Optimal predator to prey size ratios of $\text{SR} = 1, 2, 5,$ and 10 and trade-offs for the maximum uptake rate functions of $\tau = 0.5, 2, 4,$ and 8 were tested for the standard settings (Fig. 3). As SR and τ have a strong effect on the food web structure, we present results for other varied parameters for $\text{SR} = 5$ and 10 and for $\tau = 0.5$ and 4 (Figs. 5, 6, 7, 8).

The prey spectrum width SW was varied between 1, 2, and 4 size classes around the prey with optimal SR. Per default, an SW of 1 was used, assuming that the predators have a relatively narrow range of optimal prey size.

The nutrient regime was varied by changing the total phosphorous content in the system from 500 via 1,000 to 5,000 nmol-P L^{-1} (Fig. 5). The default load of 500 nmol-P L^{-1} represents oligotrophic conditions as found, for example, in the Sargasso Sea (Guildford and Hecky 2000), whereas 5,000 nmol-P L^{-1} is considered to be eutrophic.

The yield from phagotrophic predation was varied from 0.1 via 0.3 to 0.6 (Fig. 6). The yield of 30 % is considered to be standard (Pomeroy and Wiebe 1988).

The size dependencies of the cell mass-specific maximum uptake rates for DIP (V_{maxDIP}) and prey (V_{maxprey}) were tested for a quadratic loss with increasing cell radius (V_{maxDIP} and $V_{\text{maxprey}} \propto r^{-2}$), a linear decrease (V_{maxDIP} and $V_{\text{maxprey}} \propto r^{-1}$), and a linear increase (V_{maxDIP} and $V_{\text{maxprey}} \propto r$) (Fig. 7). Per default, the decrease is considered to be linear with the cell radius (Armstrong 2008).

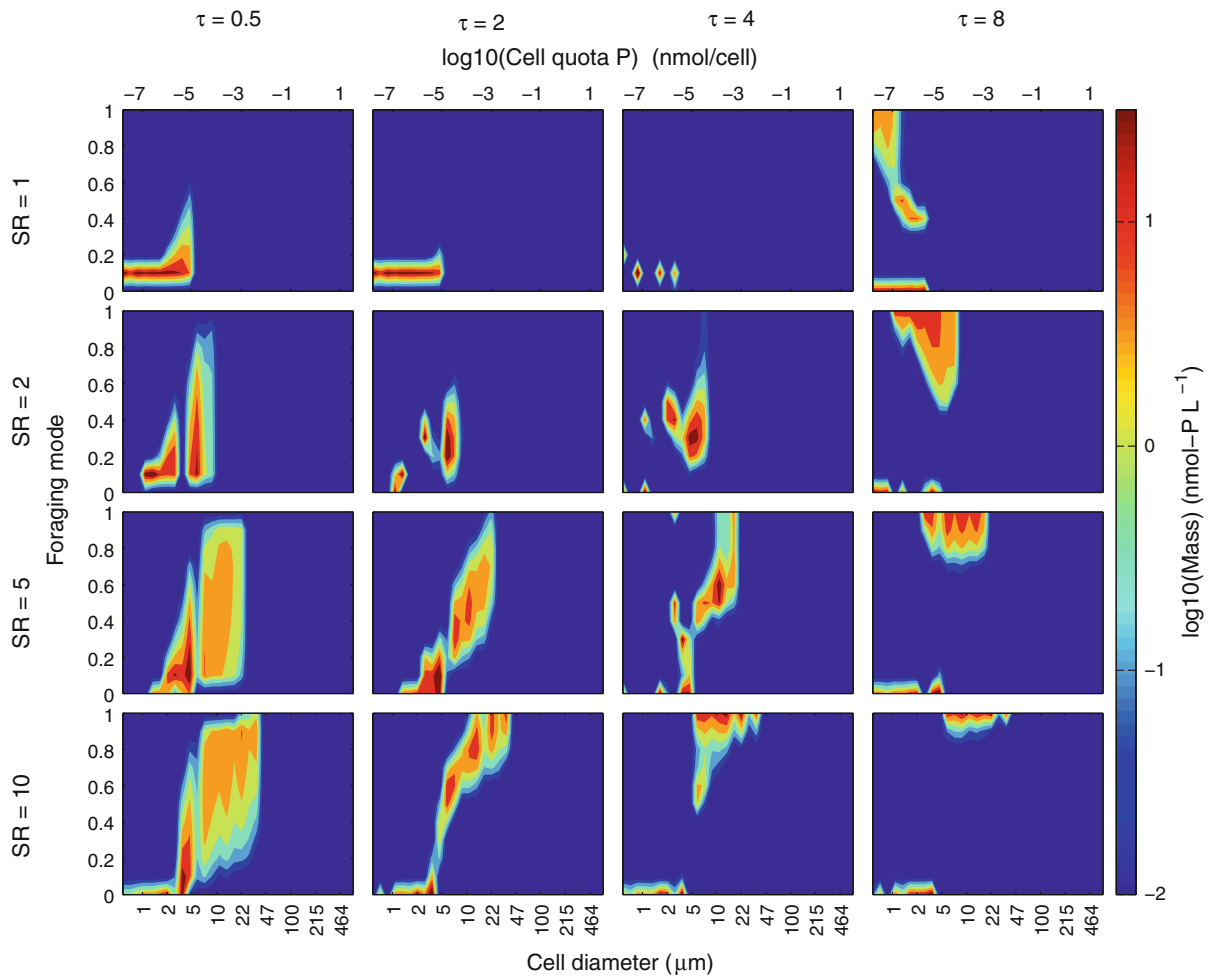


Fig. 3 Dependence of community cell size and foraging mode structure on optimal predator to prey size ratio (SR) and trade-off between osmotrophic and phagotrophic foraging mode (τ).

Other parameters as given in Table 2. A foraging mode of 1 implies strict phagotrophy, whereas a foraging mode of 0 implies strict osmotrophy

The size dependencies of cell mass-specific nutrient affinity (α) and clearance rate (β) were tested analogously to V_{max} , i.e., $\alpha, \beta \propto r^{-2}$, $\alpha, \beta \propto r^{-1}$, and $\alpha, \beta \propto r$ (Fig. 8). The latter condition (linear increase with radius) mimics strategies where organisms decouple the cell volume from cell quota (e.g., by use of vacuoles), whereas per default, the decrease is assumed to be quadratic with the cell radius (Tambi et al. 2009). The maximum prey uptake rate in our model for the smallest predators is similar to values found in a literature review by Vaqué et al. (1994). Lower prey uptake rates are found in the literature (e.g., Hansen et al. 1997), but halving the maximum prey uptake rate did not change the model results (not shown).

Stability and sensitivity to initial conditions

The final food web structures were generally established by the middle of the simulation time. The standard deviation of the mass distribution in the last year was plotted to check the stability of the emerged food web structure. The standard deviations were near zero for regions outside the mean of the established populations and generally small within the established populations (not shown). This indicates that the results are stable in the long term. Initializing the 32×11 compartments with a non-uniform mass distribution (random assignment of starting mass for each compartment within a limit of $\pm 10\%$ of the default average mass) in a limited set of simulations did not

Fig. 4 Effect of the prey spectrum width SW around the prey with optimal SR on microbial community structure. Examples are shown for SR = 5 and 10 and $\tau = 0.5$ and 4. Other parameters as given in Table 2

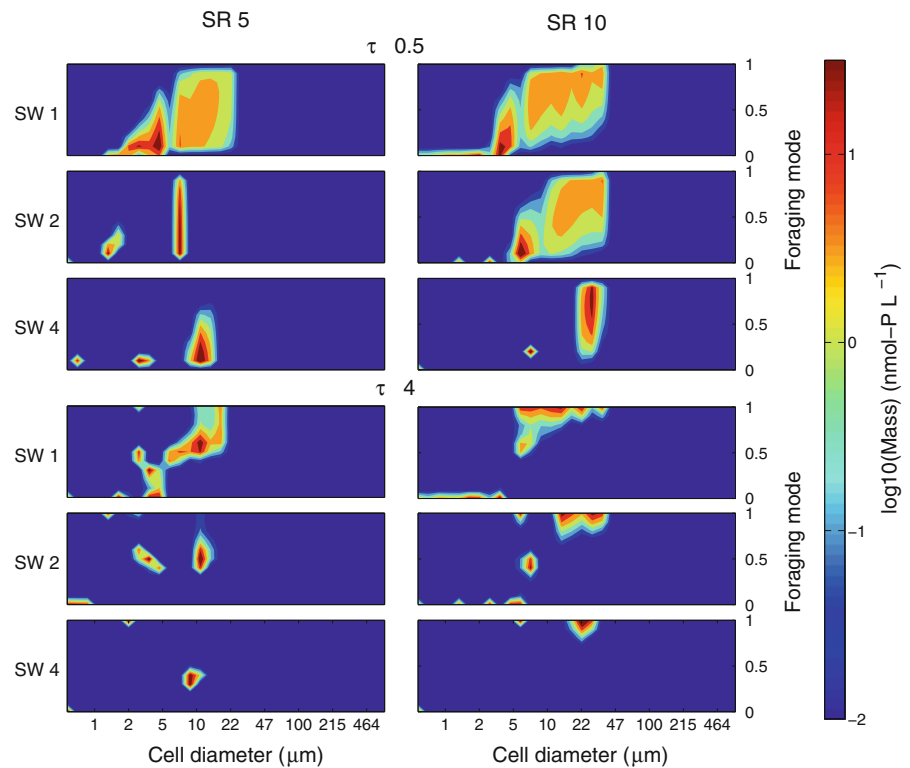


Fig. 5 Effect of the total nutrient concentration in the system on the microbial community structure. Examples shown for SR = 5 and 10 and $\tau = 0.5$ and 4. Other parameters as given in Table 2

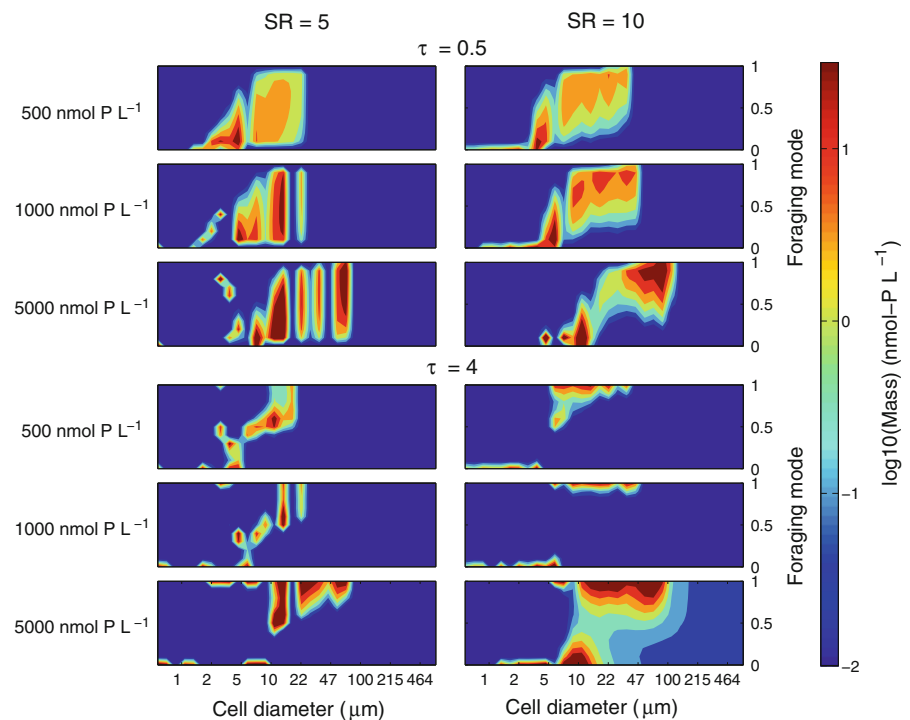


Fig. 6 Effect of the yield from predation on the microbial community structure. Examples shown for SR = 5 and 10 and $\tau = 0.5$ and 4. Other parameters as given in Table 2

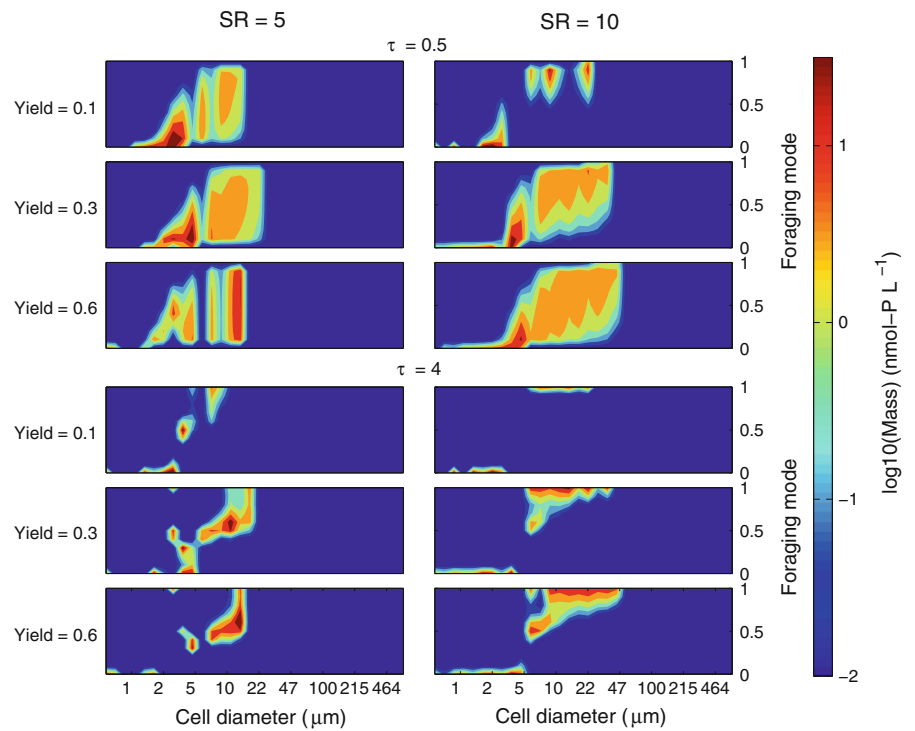


Fig. 7 Effect of the cell size dependency of the maximum uptake rates V_{max} on the microbial community structure. Examples shown for SR = 5 and 10 and $\tau = 0.5$ and 4. Other parameters as given in Table 2

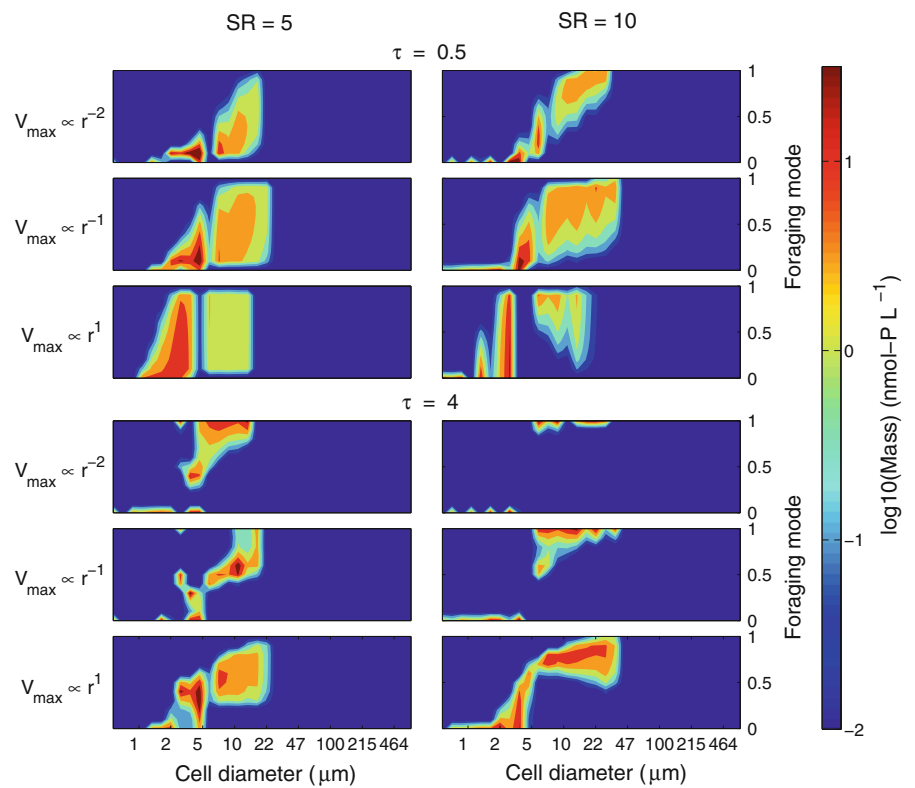
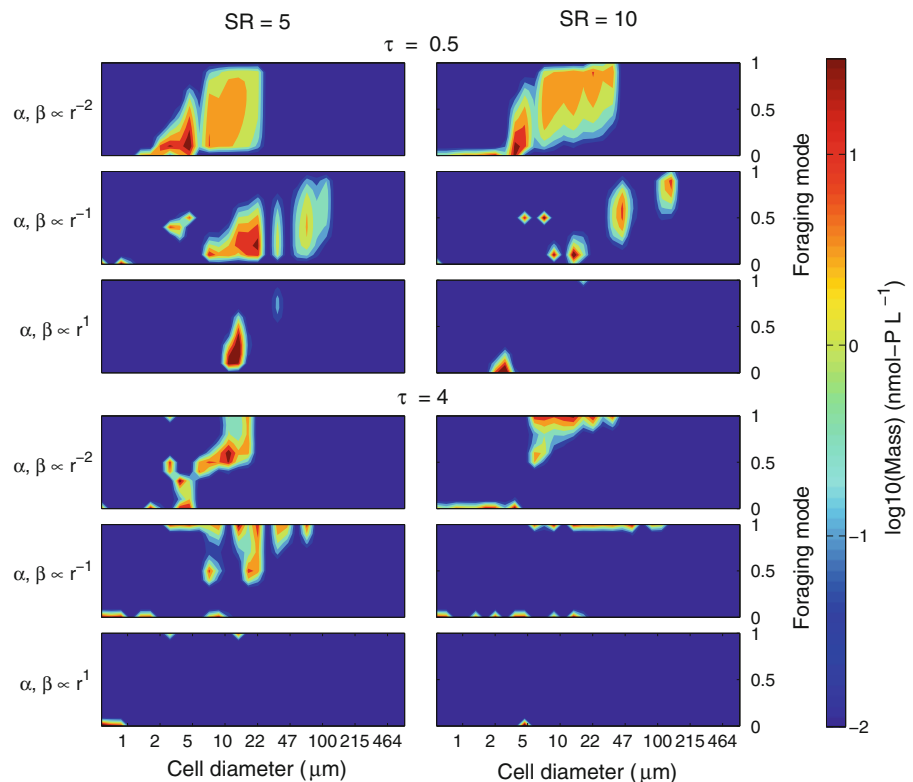


Fig. 8 Effect of the cell size dependency of the nutrient affinity α and the clearance rate β on microbial community structure. Examples shown for SR = 5 and 10 and $\tau = 0.5$ and 4. Other parameters as given in Table 2



affect the emerging food web structure (not shown), further illustrating the robustness of the emerging structures. The variations of selected parameters in the range of roughly 50–200 % of the default values, and in particular cases in the range of orders of magnitude, illustrate the sensitivity of the food web structure to chosen parameter values as presented below.

Results

On the large scale, the successfully populated areas fall within a relatively consistent region within the cell size-foraging mode plane for all simulations (Figs. 3, 4, 5, 6, 7, 8). In particular, the size range between about 1 and 20 μm was most frequently occupied by a band ranging from pure osmotrophs to phagotrophs, with a tendency of osmotrophs being smaller and phagotrophs being larger due to the given SR.

Apart from this general congruence in viable space in the cell size-foraging mode plane, however, there are conspicuous differences in the areas that are successfully populated after 10 years of simulation, depending on the parameter settings used. Generally,

mixotrophic diversity and abundance are highest at a small trade-off parameter τ , where maximum uptake rates of mixotrophs exceed those of specialist. Interestingly, however, mixotrophs normally coexist with foraging specialists even when τ is high, meaning that reduced maximum uptake rates relative to specialists still render mixotrophs successful competitors. Only at combined high SR and high τ , foraging specialists occasionally outcompete mixotrophs. A small trade-off parameter is generally necessary for mixotrophs to completely outcompete specialists, although when the optimal prey size equaled the size of the predator (SR = 1), mixotrophs outcompete specialists even at $\tau > 1$. A detailed description and explanations for the effects of different parameters on the emergent food web structure follow below. Implications of these results are given in the “Discussion” section.

Effect of trade-off parameter and optimal predator to prey size ratio

Among the tested parameters, the trade-off between osmotrophic and phagotrophic foraging and the SR have a particularly strong effect on the food web

structure and survival of mixotrophs (Fig. 3). In general, increasing τ decreases the success of mixotrophs for all SRs, whereas predominantly osmotrophic mixotrophs are especially strongly affected (Fig. 3, left to right). This follows directly from the loss in one foraging strategy outweighing the gain in the other foraging strategy when $\tau > 1$ (Fig. 1b). In contrast, at $\tau < 1$, mixotrophs are generally very successful, frequently outcompeting specialists. This is because the combined maximum uptake rates of mixotrophs for DIP and prey exceed the maximum uptake rates of specialists at $\tau < 1$ (Fig. 1b). Pure phagotrophs are most often outcompeted by mixotrophs at $\tau < 1$ (Figs. 3, 4, 5, 6, 7, 8).

The effect of SR on the survival of mixotrophs depends on τ . At $\tau = 0.5$, where mixotrophic maximum uptake rates exceed those of specialists, mixotrophs become increasingly successful with increasing SR. This results in a broad band of mixotrophs ranging from nearly pure osmotrophs to nearly pure phagotrophs, spanning cell diameters from about 5 to 50 μm for SR = 10 (Fig. 3, left). At $\tau = 8$, when cost of mixotrophy is high, mixotrophs become less successful with increasing SR. This leads to a bipolar food web structure with osmotrophic specialists of about 0.5–5 μm diameters and phagotrophic specialists of about 5–50 μm diameters, with phagotrophs preying on the osmotrophs (Fig. 3, right). The differences in cell size between established predator and prey populations are given by the SR. Generally, increasing SR increases the cell size of phagotrophs for all values of τ due to the increased size difference between the smallest available prey and the predators that can eat this prey.

Remarkably, for SR = 1 and τ up to 4, predominantly osmotrophic mixotrophs completely outcompete specialists, despite the reduced maximum uptake rates of mixotrophs relative to the specialists. Also, a SR of 1 at $\tau = 8$ is the only case where the smallest cells in the system can maintain a purely phagotrophic foraging strategy, as these phagotrophs can graze on the equally sized, smallest prey. The complete dominance of mixotrophs at SR = 1 at both low and high τ indicates that ‘eating your competitor’ (Thingstad et al. 1996) is a highly successful strategy when predators are of equal size as their prey. For SR = 2 at $\tau = 4$, mixotrophs with balanced osmotrophic and phagotrophic foraging behaviors dominate the community (Fig. 3, top left and center).

Effect of prey spectrum width SW

Besides SR, the size-dependent prey spectrum width SW strongly influences the structure of the established food web. Generally, mixotrophs profit from a less size-restricted predation range given by an increased SW (Fig. 4). At $\tau = 0.5$, relatively large mixotrophs with balanced osmotrophic and phagotrophic foraging behavior dominate the microbial community at SW = 4, completely outcompeting specialists (Fig. 4, top). Also at high cost of mixotrophy ($\tau = 4$), mixotrophs with balanced osmotrophic and phagotrophic foraging behavior generally become more dominant with increasing SW. An exception occurs for SR = 10 and SW = 4, where mixotrophs are outcompeted and a population of relatively large phagotrophs dominates in abundance, preying on smaller phagotrophs, which themselves predate on small osmotrophs (Fig. 4, lower right).

Conspicuously, an increased SW reduces the number of bands of coexisting populations observed in the size dimension, while restricting the remaining populations to a narrow range in the foraging mode and cell size dimensions. This is due to fewer distinct predation niches when the prey range is less narrowly defined in terms of prey size.

Effect of nutrient regime

Increasing the total nutrient concentration in the system up to 5,000 nmol-P L⁻¹ allows larger cells to survive, as excess DIP not used by the smaller and more competitive, top-down controlled cells becomes available. Also, as a direct consequence of the increased nutrient load, the biomasses in the established populations increase (Fig. 5).

At $\tau = 0.5$, when maximum uptake rates of mixotrophs exceed those of specialists (Fig. 5, upper half), mixotrophic strategies ranging from almost pure osmotrophy to almost pure phagotrophy become equally successful with increasing nutrient loads for SR = 5 (compared to predominantly osmotrophic mixotrophs being most successful at low nutrient concentrations). The relative increase in predominantly phagotrophic populations at increased nutrient loads both at low and high τ is explicable by channeling of the extra biomass to higher trophic levels due to top-down control of lower trophic levels. Also for SR = 10, predominantly phagotrophic mixotrophs become favored relative to lower nutrient

concentrations. In particular, two bands of medium sized ($\approx 10 \mu\text{m}$) and large (almost $100 \mu\text{m}$) mixotrophs dominate the food web at $5,000 \text{ nmol-P L}^{-1}$. Mixotrophs with balanced osmotrophic and phagotrophic foraging are outcompeted in this case because their combined maximum uptake rates are much lower than either those of more specialized mixotrophs or pure specialists (Fig. 1). For $\text{SR} = 5$, mixotrophs are generally more successful than foraging specialists at intermediate and high nutrient loads when the trade-off parameter is low.

Similarly as at $\tau < 1$, predominantly phagotrophic mixotrophs and pure phagotrophs are favored with increasing nutrient concentrations at $\tau = 4$ for $\text{SR} = 5$ (Fig. 5, lower half). Eutrophication ($5,000 \text{ nmol-P L}^{-1}$) at $\tau = 4$ for $\text{SR} = 10$ is the only case where some of the largest cells (over $600 \mu\text{m}$) can persist in our simulations. Also, it is a rare case where all intermediate mixotrophic degrees can coexist with specialists at a high cost of mixotrophy even when $\text{SR} = 10$ (Fig. 5, lower right).

Effect of yield

A low yield from predation generally disfavors mixotrophs, in particular those with predominantly phagotrophic foraging behavior (Fig. 6). This is true both when maximum uptake rates of mixotrophs exceed those of specialists ($\tau = 0.5$) and when cost of mixotrophy is high ($\tau = 4$). The reduced success of phagotrophic strategies when the yield is low is directly related to less efficient predation. A high yield at $\tau = 0.5$ increases the success of relatively large cells ($10\text{--}20 \mu\text{m}$) of any mixotrophic degree for $\text{SR} = 5$, and mixotrophs outcompete all but the smallest specialists in this case. At the same time, a high yield reduces the success of smaller and predominantly osmotrophic mixotrophs for $\text{SR} = 5$. For $\text{SR} = 10$, the predominantly osmotrophic mixotrophs remain most successful, likely because mixotrophic predation of direct competitors, from which largely phagotrophic mixotrophs benefit at $\text{SR} = 5$, is less efficient for $\text{SR} = 10$ (Fig. 6, upper half).

A high yield at $\tau = 4$ favors pure phagotrophs for both $\text{SR} = 5$ and 10 . Also, mixotrophs of balanced osmotrophic and phagotrophic foraging behavior become more competitive with increasing yield at high cost of mixotrophy (Fig. 6, lower half).

Effect of size dependency of maximum uptake rates V_{max}

Increasing maximum uptake rates relative to cell size (from a quadratic loss of V_{max} with cell size to the default linear decrease and a linear increase with cell size) generally favors predominately phagotrophic mixotrophs and pure phagotrophs both at low and high τ (Fig. 7). This shift in abundance to more phagotrophic strategies may occur because larger cells benefit when the maximum uptake rates are positively related with cell size. Large cells are typically (partly) phagotrophic in our system due to the SRs exceeding 1.

An increased size penalty of the maximum uptake rates such that V_{max} decreases quadratically with the cell radius, combined with a high cost of mixotrophy, is one of the few cases in our simulations where mixotrophs of any degree are completely outcompeted by osmotrophic and phagotrophic specialists (Fig. 7, lower half, top right). This defeat of mixotrophs may be explained by their reliance on partly phagotrophic foraging, which implies that mixotrophs must be larger than pure osmotrophs when SR exceeds 1. The thereby experienced strong size penalty in terms of maximum uptake rates, combined with the high cost of mixotrophy in general, probably renders mixotrophy non-viable in this case.

Effect of size dependency of nutrient affinity α and clearance rate β

Reducing the size penalty of α and β ($\alpha, \beta \propto r - 1$) and alleviating the penalty all together such that α and β increase linearly with cell size ($\alpha, \beta \propto r$) lead to more distinct, separate populations on the foraging mode–cell size plane (Fig. 8). Thanks to the reduced size penalty, larger cells of up to $100 \mu\text{m}$ persist when α and β decrease linearly instead of quadratically with the square of the cell radius.

At $\tau = 0.5$, isolated populations of mixotrophs almost completely outcompete specialists with reduced size penalty (Fig. 8, upper half, middle). For a linear increase of α and β with size, predominately osmotrophic mixotrophs of about $10 \mu\text{m}$ outcompete specialists for $\text{SR} = 5$, whereas only pure osmotrophs survive for $\text{SR} = 10$ (Fig. 8, upper half, bottom). At a high cost of mixotrophy ($\tau = 4$), reducing the size penalty of α and β or alleviating the penalty all together strongly disfavors mixotrophs for $\text{SR} = 5$

and 10 (Fig. 8, lower half). Similar as in the case described above for V_{\max} , this is probably because at reduced or alleviated size penalty, large cells can establish. Hence, in addition to the disadvantage of mixotrophs in terms of maximum uptake rates relative to specialists when $\tau > 1$, the general penalty for biomass-specific maximum uptake rates becomes heavier as cells are larger. The combined penalty for mixotrophs in this case may render them non-viable, with the result that the food web consists of isolated populations of pure osmo- and phagotrophs, whose cell size differences are given by the SR.

In summary, strategies reducing or alleviating the size penalty of α and β , known to be important in nature, are here shown to have strong effects on emergent food web structures. While it is intuitive that reduced penalty allows larger cells to compete, the shown effects on mixotrophic survival are less obvious.

Discussion

A major key to the understanding of emergent aquatic food web structures and dynamics may lie in the mechanistic understanding of trade-offs between different organism traits. Regarding microbial food webs, trade-offs between the trophic modes and the degrees of mixotrophy in different organisms are currently hard or even impossible to measure, and they may vary within species (Stoecker 1998). Hence, the relative importance of photosynthesis, uptake of dissolved inorganic nutrients, and predation in mixotrophs (i.e., where on the foraging mode axes of the presented model the organisms are placed) is often unknown. Nevertheless, the model presented here allows us to explore the complexity of the system, giving us insights into how different life strategies of microorganisms and system parameters may interplay and determine the structure of aquatic microbial food webs.

The prevalent success of mixotrophs, both when maximum uptake rates of mixotrophs exceed those of specialists ($\tau < 1$) and when costs of mixotrophy is high ($\tau > 1$), is a major result in our study and agrees with findings of high mixotrophic abundance in field surveys (Havskum and Riemann 1996; Zubkov and Tarran 2008; Hartmann et al. 2012). Despite of inconclusive evidence for mixotrophy trade-offs in

experiments and lack of direct measurements in nature (Rothhaupt 1996; McKie-Kriesberg et al. 2011), it is commonly assumed that there is a metabolic cost to maintain two internal foraging systems (Thingstad et al. 1996; Ward et al. 2011). Also, space conflicts for external uptake sites on the cell surface are thought to reduce growth efficiencies of mixotrophs relative to specialists (Flynn and Mitra 2009; Ward et al. 2011). This would imply that a trade-off parameter of $\tau > 1$ in the present study is most realistic. It is remarkable that mixotrophs in our simulations typically coexist with foraging specialists even at $\tau > 1$, where maximum uptake rates of specialists exceed the combined maximum uptake rates for DIP and prey of mixotrophs. This suggests that benefits of mixotrophy could potentially outweigh high costs arising from mixotrophic foraging behavior in nature. Notably, at high τ , mixotrophs with balanced osmotrophic and phagotrophic foraging behavior (f around 0.5) were typically more rare than predominantly osmotrophic and phagotrophic mixotrophs. The competitive disadvantage of balanced mixotrophs arrives from the trade-off functions (Fig. 1b), where combined maximum uptake rates of DIP and prey of mixotrophs with foraging modes around 0.5 are much smaller than combined maximum uptake rates of more specialized mixotrophs when τ exceeds 1. This result is consistent with previous observations that most mixotrophs in nature seem to be predominantly osmotrophic or phagotrophic (Stoecker 1998). Interestingly, however, our model also supports balanced mixotrophic strategies at high costs of mixotrophy under conditions where efficient predation on competitors is favored, such as when SR is small (Fig. 3), predation yield is high (Fig. 6), or the prey spectrum width SW is wide (Fig. 4).

On the other hand, mixotrophs most strongly dominate in our model and cover a wider range of foraging modes and cell sizes when $\tau < 1$. The increased maximum uptake rates of mixotrophs relative to specialists in these scenarios clearly favor a high diversity of mixotrophs in the emergent food webs. Knowing that mixotrophy is a highly diverse and widely spread strategy that frequently dominates in a variety of aquatic systems (e.g., Havskum and Riemann 1996; e.g., Burkholder et al. 2008; e.g., Hartmann et al. 2012), this may imply that costs of mixotrophy in nature are actually smaller than previously assumed. Our model results for $\tau < 1$ are in fact

consistent with the hypothesis that mixotrophy not only is free of extra costs, but may even come with a “bonus” relative to specialized foraging.

From an evolutionary point of view, mixotrophy can be considered the primordial form of foraging in eukaryotic phytoplankton. Chloroplasts in phytoplankton are derived from photosynthetic cyanobacteria that were taken up as primary endosymbionts by primordial phagotrophic eukaryotes (Falkowski et al. 2004). While additional secondary and tertiary endosymbioses occurred in several lineages later on, phagotrophic abilities may or may not have been given up by the phytoplankton. Assuming that phagotrophic abilities infer little cost, phytoplankton loosing their primordial phagotrophic abilities would have experienced little selective advantage compared to those keeping them. Indeed, maintaining the photosynthetic apparatus requires several-fold more energy than maintaining the feeding apparatus in mixotrophs (Stoecker 1998). Realizing that mixotrophic species are found in most phytoplankton lineages, perhaps only with the exception of diatoms (Flynn et al. 2013), these findings support the notion that mixotrophs (those phytoplankton that kept phagotrophic abilities) may have little disadvantage in terms of energy requirements, at least relative to pure osmotrophs who gave up on phagotrophic abilities (Stoecker 1998). Nevertheless, direct experimental data to support or refute the hypothesis that mixotrophy may in fact come with a “bonus” relative to specialized foraging under a variety of conditions are still lacking. Further experimental research and understanding of mixotrophic physiology is required to formulate a more conclusive explanation on the success of mixotrophs in aquatic environments.

The size of the successful microorganisms in our model (≈ 0.5 – $100 \mu\text{m}$) overlaps with the sizes of bacteria (≈ 0.2 – $2 \mu\text{m}$), nanoflagellates (≈ 2 – $20 \mu\text{m}$), and larger dinoflagellates and ciliates (up to $100 \mu\text{m}$ and larger). Most often, mixotrophic populations in our model fall into the size range from 2 to $10 \mu\text{m}$, reflecting natural populations of mixotrophic nanoflagellates of similar size, which are highly abundant in both coastal areas (Havskum and Riemann 1996) and oligotrophic gyres (Sanders et al. 2000; Zubkov and Tarran 2008; Hartmann et al. 2012). Data from a P-enrichment experiment in the ultra-oligotrophic Eastern Mediterranean (Krom et al. 2005) are consistent with the idea that nanoflagellates also actively

perform mixotrophy in this system. Following P-addition, phytoplankton did generally not show a response due to P and N co-limitation (Pitta et al. 2005; Zohary et al. 2005). However, pigmented nanoflagellates in the size range of 10 – $20 \mu\text{m}$, many identified as prymnesiophytes, showed a slight increase in biomass (Psarra et al. 2005). This seems only explicable by mixotrophic foraging on bacteria, which were stimulated by P-addition (Zohary et al. 2005).

Larger mixotrophs (around $100 \mu\text{m}$) persisted in our model in high nutrient regimes, independently of their foraging strategy. This confirms theoretical predictions of larger mixotrophs and a broader plankton size spectrum when nutrients are replete (Chisholm 1992; Ward et al. 2011). High nutrient concentrations favoring large cells can be explained by a strong grazing control of smaller individuals. When the total nutrient content in the system increases, excessive resources that are not used by top-down controlled smaller cells will become available, allowing larger, competitively inferior but defensively superior cells to establish. This is consistent with blooming of large phytoplankton in nutrient rich conditions. Large mixotrophs in the highest nutrient settings of our model match with high abundances of large mixotrophic ciliates and dinoflagellates in coastal waters and harmful algal blooms (Stoecker 1999; Stoecker et al. 1989; Burkholder et al. 2008; Sanders 2011). These ecologically feasible findings promote confidence on the biological meaningfulness of our model settings and results.

It is interesting to observe that mixotrophs occasionally outcompete specialists in our model when SR is sufficiently small. A small SR means that the prey is of similar size as the predator, making the prey a direct competitor of the predator. This is consistent with the hypothesis that ‘eating your competitor’ (Thingstad et al. 1996) is a key for the success of mixotrophs. The fact that relatively small, predominantly osmotrophic mixotrophs completely outcompete specialists at $\tau > 1$ when $\text{SR} = 1$ (Fig. 3) makes this point very clear. Even though the maximum uptake rates of the mixotrophs are smaller compared to their specialized competitors in this case, the mixotrophs manage to suppress pure osmotrophs by foraging on them. The other case in our simulations where mixotrophs completely outcompete specialists is at a high SW, here even for high SR although at $\tau < 1$ (Fig. 4). The explanation for mixotrophic dominance in this case

may be similar as for small SR, since a high SW facilitates predation on competitors of similar sizes even when SR is high.

Size structure in plankton models is important to simulate realistic food web dynamics (Moloney and Field 1991). Optimal SRs are typically assumed to be on the order of 10:1 in planktonic food webs (.g. Azam et al. 1983), whereas in reality, optimal SRs differ widely between groups. Dinoflagellates can, for example, ingest prey of up to equal size or larger than themselves (Hansen et al. 1994). Large SR forces phagotrophs to increase in size in order to predate optimally on the available prey. Hence, common modeling practice of fixing SR may strongly bias the emergent food web structures and dynamics. The weakened competitiveness of mixotrophs at high SR is understandable from the increased size penalty of maximum uptake rates when cell sizes increase, which acts in addition to reduced maximum uptake rates of mixotrophs relative to specialists at $\tau < 1$. Again, increased size differences between prey and predator at large SR also reduce efficient removal of direct competitors through mixotrophic predation.

The prey spectrum width SW influences the banding of established populations in the size dimension of our model (Fig. 4). Since a narrower SW supports a large number of different prey size-specific niches, a large number of population bands with distinct cell sizes are maintained. Highly specialized predation at low SW also allows closely resembling populations to coexist, cumulatively covering a broad range of cell sizes and mixotrophic foraging modes in the cell size-foraging mode plane. In contrast, at wide SW, the overlap of common prey in adjacent populations is large. Hence a few, competitively superior populations monopolize the available resources, restricting the food web to a few confined populations in the cell size-foraging mode plane. Conclusively, the model simulations suggest that a more detailed knowledge of both SR and SW in natural populations has the potential to explain much of the subtle structures in aquatic microbial food webs.

Foraging kinetics and the role of cell size

The functional responses used in our study (Fig. 1a) are typical in aquatic microbial food webs (Taylor 1978; Fenchel 1982; Bjørnson and Kuparinen 1991), and the maximum prey uptake rate in our model for the smallest

predators is similar to values found in a literature review by Vaqué et al. (1994). Lower prey uptake rates are found in the literature (e.g. Hansen et al. 1997), but halving the maximum prey uptake rate did not change the model results (not shown). The default maximum nutrient affinity for pure osmotrophs and the maximum clearance rate for pure phagotrophs used in our model are similar to values suggested in Lignell et al. (2013). The minimum generation time of 6 h for pure osmotrophs, which follows from their maximum phosphorous uptake rate, matches with values found for pelagic bacteria in oligotrophic systems (Kemp et al. 1993). Halving or doubling the maximum nutrient affinity (α_0) and clearance rate (β_0) only slightly affected the food web structure (not shown).

In general, mass specific maximum uptake rates decrease with increasing size of the organisms (Friebele et al. 1978; Raven 1998; Armstrong 2008), but the nutrient regime may influence the exact relationship between the maximum uptake rate and the cell size. Aksnes and Cao (2011) argue for a quadratic decrease in the mass-specific uptake rate with cell radius in oligotrophic conditions, whereas they predict a linear decrease in eutrophic conditions. However, the relationship is not always clear (Banse 1982), and volume-specific uptake rates can increase with size, depending on the groups that are compared (Irwin et al. 2006). Varying the size dependency of the maximum uptake rates according to these scenarios as demonstrated in this study illustrates the negative effect of a strong size penalty on mixotrophs (Fig. 7).

Cell size is known to be a master trait influencing the growth rate, but handling time and porter density additionally influence maximum uptake rates and nutrient affinities (Aksnes and Cao 2011; Fiksen et al. 2013). Since detailed knowledge about handling time and nutrient porter densities are still lacking, we have not explicitly included these parameters in our model. However, the trade-off function for the maximum uptake rates can be interpreted as a representation of trade-offs that may be associated with handling time and porter densities for mixotrophs.

The decrease in nutrient affinities and clearance rates with the square of the radius follows from diffusion limited uptake at low resource concentrations and the assumption that the cell concentration of the limiting element is constant (Jumars et al. 1993; Tambi et al. 2009). That there are other, larger phytoplankton in the ocean than cyanobacteria is not

only because of predation pressure, but also because they have found ways to reduce this size penalty. Increasing cell size with vacuoles filled with non-limiting resources allows, for example, diatoms and some large bacterioplankton to escape the strong size penalty for nutrient affinities, while at the same time becoming better protected against predation (Thingstad et al. 2005b). Larger cells persisting when α and β decrease linearly instead of quadratically with the cell radius in our model (Fig. 8) confirm this benefit of increased size. The problem of omitting the strong size penalty has probably been dealt with since at least the Ediacaran about 600–500 million years ago (Laflamme et al. 2009).

Applicability of our model to different environments

There is no intrinsic property in our model that restricts its applicability to marine oligotrophic systems. Although oligotrophy is a typical state of vast areas of the pelagic ecosystem (Maranon et al. 2003), it may also apply to freshwater systems (Suttle and Harrison 1988), where mixotrophy is known to be an important strategy among microorganisms (Sanders 1991). Eutrophic conditions such as eutrophic lakes or marine upwelling regions may also be studied with our model by adjusting the total nutrient content in the system.

In mineral nutrient limited environments, phagotrophic foraging can supply necessary mineral nutrients in the form of prey particles, giving mixotrophs an advantage over osmotrophic specialists. Whereas mineral nutrient limitation and competition for mineral nutrients often occur in aquatic ecosystems, in particular in pelagic environments, mixotrophs competing for energetic carbon sources also occur in light-limited environments (Jones 1997). When the environment is light limited, obtaining energy (organic carbon) through phagotrophic feeding may be crucial and responsible for the survival of microalgae in the Arctic winter (Zhang et al. 1998). Light-limitation is not considered in our model and should be subject to future studies. Hence, the present analysis relates to oligotrophic but light replete environments such as the ultraoligotrophic Eastern Mediterranean (Thingstad et al. 2005a), the vast subtropical gyres (Hartmann et al. 2012) or oligotrophic lakes (Suttle and Harrison 1988; Stockner and Shortreed 1989).

Conclusions

Recent findings of the dominant role of mixotrophs as both primary producers and bacterivores in oligotrophic gyres (Hartmann et al. 2012) stress the importance of including mixotrophy in food web and large-scale climate models. Ultimately, an increased system understanding of aquatic microbial food webs and their role in biogeochemical carbon cycling can only be obtained when understanding the role and success of mixotrophy. By using a highly resolved differential equation-based model where organisms of different foraging modes and a wide range of cell sizes interact, we studied the coexistence of mixotrophs with foraging specialists and how food web structures emerge from different life strategies at the cellular level.

Unlike previous models, the high resolution in foraging mode and cell size used here give an understanding of the control of mixotrophic diversity and size structure in microbial food webs that may be applied to natural systems. Larger cells persist in eutrophic environments, and mixotrophs are successful in a wide range of settings in our model, capturing known ecological trends. Particularly successful are mixotrophs between 2 and 10 μm , reflecting naturally abundant mixotrophic nanoflagellates (Unrein et al. 2007; Zubkov and Tarran 2008; Hartmann et al. 2012). Also, predominantly osmotrophic mixotrophs often dominate the microbial community in our model, confirming previous modeling studies where primarily autotrophic mixotrophs were most successful (Thingstad et al. 1996; Crane and Grover 2010). We confirm the prediction that large mixotrophs are successful when nutrients are replete (Ward et al. 2011).

The emerging food web structure is highly sensitive to SR and SW. These size-dependending parameters define a viable range of cell sizes for coexisting populations and lead to a banding of the food web structure in the size dimension. Furthermore, they strongly influence the success of mixotrophs among foraging specialists. Notably, mixotrophs outcompete specialists most often when SR is sufficiently small and when SW is large. The optimal foraging on prey of one's own size and a wider selection of suitable prey sizes even when SR is large at large SW enhances an efficient removal of direct competitors. Hence, simulations of this study confirm that 'eating your competitor' (Thingstad et al. 1996) is indeed a key for the success of mixotrophs.

Besides SR and SW, the foraging mode trade-off significantly influences the food web structure, in particular with respect to abundance and diversity of mixotrophs. The fact that mixotrophs successfully coexist with foraging specialists even at trade-off parameters larger than one indicates that the benefits of mixotrophic foraging may outweigh potential high costs of maintaining two nutritional systems in nature. On the other hand, success and diversity of mixotrophs was largest in our model when τ was smaller than one. Closely matching the high abundance of mixotrophs in different aquatic environments, these results at $\tau < 1$ support the hypothesis that mixotrophy may come with a “bonus” relative to specialized foraging.

The results of this study encourage further experimental work and development of observational techniques to improve measurements of the degree of mixotrophy and trade-offs in natural microbial food webs. This will be crucial for a more clear understanding of the prevalent success of mixotrophs and its underlying physiological and environmental mechanisms. Also, the study demonstrates that an insufficient resolution in cell size and foraging mode as well as size-dependent model parameters can strongly bias model dynamics, thus promoting an inclusion of different cell sizes and foraging modes in future biogeochemical modeling studies.

Acknowledgments The study was done as part of the MINOS project financed by EU-ERC (proj.nr 250254) and with the support of the Norwegian Research Council. We thank two anonymous reviewers for constructive comments that improved a previous version of the manuscript.

References

- Aksnes DL, Cao FJ (2011) Inherent and apparent traits in microbial nutrient uptake. *Mar Ecol Prog Ser* 440:41–51
- Armstrong RA (2008) Nutrient uptake rate as a function of cell size and surface transporter density: a Michaelis-like approximation to the model of Pasciak and Gavis. *Deep Sea Res I* 55:1311–1317
- Azam F, Fenchel T, Field JG, Gray JS, Meyer-Reil LA, Thingstad F (1983) The ecological role of water-column microbes in the sea. *Mar Ecol Prog Ser* 10:257–263
- Banse K (1982) Cell volumes, maximal growth rates of unicellular algae and ciliates, and the role of ciliates in the marine pelagial. *Limnol Ocean* 27:1059–1071
- Baretta-Bekker JG, Baret JW, Hansen AS, Riemann B (1998) An improved model of carbon and nutrient dynamics in the microbial food web in marine enclosures. *Aquat Microb Ecol* 14:91–108
- Bjørnsen PK, Kuparinen J (1991) Growth and herbivory by heterotrophic dinoflagellates in the Southern Ocean, studied by microcosm experiments. *Mar Biol* 109:397–405
- Burkholder JM, Gilbert PM, Skelton HM (2008) Mixotrophy, a major mode of nutrition for harmful algal species in eutrophic waters. *Harmful Algae* 8:77–93
- Castellani M, Våge S, Strand E, Thingstad F, Giske J (2012) The scaled subspaces method: a new trait-based approach to model communities of populations with largely inhomogeneous density. *Ecol Mod*. doi:10.1016/j.ecolmodel.2012.12.006
- Chisholm SW (1992) Primary productivity and biogeochemical cycles in the sea. Plenum Press, Berlin, pp 213–237
- Crane KW, Grover JP (2010) Coexistence of mixotrophs, autotrophs, and heterotrophs in planktonic microbial communities. *J Theor Biol* 262:517–527
- Falkowski PG, Katz ME, Knoll AH, Quigg A, Raven JA, Schofield O, Taylor FJR (2004) The evolution of modern eukaryotic phytoplankton. *Science* 305:354–360
- Fenchel T (1982) Ecology of heterotrophic microflagellates. II. Bioenergetics and growth. *Mar Ecol Prog Ser* 8:225–231
- Fiksen Ø, Follows MJ, Aksnes DL (2013) Trait-based models of nutrient uptake in microbes extend the Michaelis–Menten framework. *Limnol Ocean* 58:193–202
- Flynn KJ, Mitra A (2009) Building the “perfect beast”: modelling mixotrophic plankton. *J Plankton Res* 31:965–992
- Flynn KJ, Stoecker DK, Mitra A, Rave JA, Glibert PM, Hansen PJ, Graneli E, Burkholder JM (2013) Misuse of the phytoplankton–zooplankton dichotomy: the need to assign organisms as mixotrophs within plankton functional types. *J Plankton Res* 35:3–11
- Friebele ES, Correl DL, Faust MA (1978) Relationship between phytoplankton cell size and the rate of orthophosphate uptake: in situ observations of an estuarine population. *Mar Biol* 45:39–52
- Guildford SJ, Hecky RE (2000) Total nitrogen, total phosphorus, and nutrient limitation in lakes and oceans: is there a common relationship?. *Limnol Ocean* 45:1213–1223
- Hammer AC, Pitchford JW (2005) The role of mixotrophy in plankton bloom dynamics, and the consequences for productivity. *ICES J Mar Sci* 62:833–840
- Hansen B, Bjørnsen PK, Hansen PJ (1994) The size ratio between planktonic predators and their prey. *Limnol Ocean* 39:395–403
- Hansen PJ, Bjørnsen PK, Hansen BW (1997) Zooplankton grazing and growth: scaling within the 2–2,000- μm body size range. *Limnol Ocean* 42:687–704
- Hartmann M, Grub C, Tarran GA, Martin AP, Burkill PH, Scanlan DJ, Zubkov MV (2012) Mixotrophic basis of Atlantic oligotrophic ecosystems. *PNAS USA* 109:5756–5760
- Havskum H, Riemann B (1996) Ecological importance of bacterivorous, pigmented flagellates (mixotrophs) in the Bay of Aarhus, Denmark. *Mar Ecol Prog Ser* 137:251–263
- Irwin AJ, Finkel ZV, Schofield OME, Falkowski PG (2006) Scaling-up from nutrient physiology to the size-structure of phytoplankton communities. *J Plankton Res* 28:459–471
- Jones RI (1997) A classification of mixotrophic protists based on their behaviour. *Freshw Biol* 37:35–43
- Jost C, Lawrence CA, Campolongo F, van de Bund W, Hill S, DeAngelis DL (2004) The effects of mixotrophy on the

- stability and dynamics of a simple planktonic food web model. *Theor Popul Biol* 66:37–51
- Jumars P, Deming J, Hill P, Karp-Boss L, Dade W (1993) Physical constraints on marine osmotrophy in an optimal foraging context. *Mar Microb Food Webs* 7:121–161
- Kemp PF, Lee S, LaRoche J (1993) Estimating the growth rate of slowly growing marine bacteria from RNA content. *Appl Environ Microbiol* 59:2594–2601
- Krom MD, Woodward EMS, Herut B, Kress N, Carbo P, Mantoura RFC, Spyres G, Thingstad TF, Wassmann P, Wexels-Riser C, Kitidis V, Law CS, Zoda G (2005) Nutrient cycling in the south east Levantine basin of the eastern Mediterranean: results from a phosphorous starved system. *Deep Sea Res II* 52:2879–2896
- Laflamme M, Xiao S, Kowalewski M (2009) Osmotrophy in modular Ediacara organisms. *PNAS USA* 106:14438–14443
- Lignell R, Haario H, Laine M, Thingstad TF (2013) Getting the “right” parameter values for models of the pelagic microbial food web. *Limnol Ocean* 58:301–313
- Litchman E, Klausmeier CA, Schofield OM, Falkowski PG (2007) The role of functional traits and trade-offs in structuring phytoplankton communities: scaling from cellular to ecosystem level. *Ecol Lett* 10:1170–1181
- Loeuille N, Loreau M, Levin SA (2005) Evolutionary emergence of size-structure food webs. *PNAS USA* 102:5761–5766
- Maranon E, Behrenfeld MJ, Gonzalez N, Mourino B, Zubkov MV (2003) High variability of primary production in oligotrophic waters of the Atlantic Ocean: uncoupling from phytoplankton biomass and size structure. *Mar Ecol Prog Ser* 257:1–11
- McKie-Kriesberg ZM, Fay SA, Sanders RW (2011) Competitive assays of two mixotrophs and two diatoms from the Ross Sea, Antarctica. *J Phycol* 47:S67–S67
- Mitra A, Flynn KJ (2010) Modelling mixotrophy in harmful algal blooms: more or less the sum of the parts? *J Mar Syst* 83:158–169
- Moloney CL, Field JG (1991) The size-based dynamics of plankton food webs. I. A simulation model of carbon and nitrogen flows. *J Plankton Res* 13:1003–1038
- Pitta P, Stambler N, Tanaka T, Zohary T, Tselepidis A, Rassoulzadegan F (2005) Biological response to P addition in the Eastern Mediterranean Sea. The microbial race against time. *Deep Sea Res II* 52:2961–2974
- Pomeroy LR, Wiebe WJ (1988) Energetics of microbial food webs. *Hydrobiologia* 159:7–18
- Psarra S, Zohary T, Krom MD, Mantoura RFC, Polychronaki T, Stambler N, Tanaka T, Tselepidis A, Thingstad TF (2005) Phytoplankton response to a Lagrangian phosphate addition in the Levantine Sea (Eastern Mediterranean). *Deep Sea Res II* 52:2944–2960
- Raven JA (1998) The twelfth Tansley lecture, small is beautiful: the picophytoplankton. *Funct Ecol* 12:503–513
- Rothhaupt KO (1996) Utilization of substitutable carbon and phosphorus sources by the mixotrophic chrysophyte *ochromonas* sp. *Ecology* 77:706–715
- Sanders RW (1991) Mixotrophic protists in marine and freshwater ecosystems. *J Eukaryot Microbiol* 38:76–81
- Sanders RW (2011) Alternative nutritional strategies in protists: symposium introduction and a review of freshwater protists that combine photosynthesis and heterotrophy. *J Eukaryot Microbiol* 58:181–184
- Sanders RW, Porter KG, Caron DA (1990) Relationship between phototrophy and phagotrophy in the mixotrophic chrysophyte *Poteriochromonas malhamensis*. *Microb Ecol* 19:97–109
- Sanders RW, Berninger UG, Lim EL, Kemp PF (2000) Heterotrophic and mixotrophic nanoplankton predation on picoplankton in the Sargasso Sea and on Georges Bank. *Mar Ecol Prog Ser* 192:103–118
- Shampine LF, Reichelt MW (1997) The matlab ODE suite. *SIAM J Sci Comput* 18:1–22
- Sheldon RW, Prakash A, Sutcliffe WH (1972) The size distribution of particles in the ocean. *Limnol Ocean* 17:327–340
- Stickney HL, Hood RR, Stoecker DK (2000) The impact of mixotrophy on planktonic marine ecosystems. *Ecol Mod* 125:203–230
- Stockner JG, Shortreed KS (1989) Algal picoplankton production and contribution to food-webs in oligotrophic British Columbia lakes. *Hydrobiologia* 173:151–166
- Stoecker DK (1998) Conceptual models of mixotrophy in planktonic protists and some ecological and evolutionary implications. *Eur J Protistol* 34:281–290
- Stoecker DK (1999) Mixotrophy among dinoflagellates. *J Eukaryot Microbiol* 46:397–401
- Stoecker DK, Taniguchi A, Michaels AE (1989) Abundance of autotrophic, mixotrophic and heterotrophic planktonic ciliates in shelf and slope waters. *Mar Ecol Prog Ser* 50:241–254
- Suttle CA, Harrison PJ (1988) Ammonium and phosphate uptake rates, N:P supply ratios, and evidence for N and P limitation in some oligotrophic lakes. *Limnol Ocean* 33:186–202
- Tambi H, Flaten GAF, Egge JK, Bødtker G, Jacobsen A, Thingstad TF (2009) Relationship between phosphate affinities and cell size and shape in various bacteria and phytoplankton. *Aquat Microb Ecol* 57:311–320
- Taylor WD (1978) Growth responses of ciliate protozoa to the abundance of their bacterial prey. *Microb Ecol* 4:207–214
- Thingstad TF, Havskum H, Garde K, Riemann B (1996) On the strategy of “eating your competitor”: a mathematical analysis of algal mixotrophy. *Ecology* 77:2108–2118
- Thingstad TF, Krom MD, Flagen GAF, Mantoura RFC, Groom S, Herut B, Kress N, Law CS, Pasternak A, Pitta P, Psarra S, Rassoulzadegan R, Tanaka T, Tselepidis A, Wassmann P, Woodward EMS, Riser CW, Zodiatis G, Zohary T (2005a) Nature of phosphorous limitation in the ultraoligotrophic Eastern Mediterranean. *Science* 309:1068–1071
- Thingstad TF, Øvreås L, Egge JK, Løvdal T, Heldal M (2005b) Use of non-limiting substrates to increase size; a generic strategy to simultaneously optimize uptake and minimize predation in pelagic osmotrophs?. *Ecol Lett* 8:675–682
- Troost TA, Kooi BW, Kooijman SALM (2005) When do mixotrophs specialize? Adaptive dynamics theory applied to a dynamic energy budget model. *Math Biosci* 193:159–182
- Unrein F, Massana R, Alonso-Sáez L, Gasol JM (2007) Significant year-round effect of small mixotrophic flagellates on bacterioplankton in an oligotrophic coastal system. *Limnol Ocean* 52:456–469

- Vaqué D, Gasol JM, Marrasé C (1994) Grazing rates on bacteria: the significance of methodology and ecological factors. *Mar Ecol Prog Ser* 109:263–274
- Ward BA, Dutkiewicz S, Barton AD, Follows MJ (2011) Biophysical aspects of resource acquisition and competition in algal mixotrophs. *Am Nat* 178:98–112
- Zhang Q, Gradinger R, Spindler M (1998) Dark survival of marine microalgae in the high Arctic (Greenland Sea). *Polarforschung* 65:111–116
- Zohary T, Herut B, Krom MD, Mantoura RFC, Pitta P, Psarra S, Rassoulzadegan F, Stambler N, Tanaka T, Thingstad TF, Woodward EMS (2005) P-limited bacteria but N and P co-limited phytoplankton in the Eastern Mediterranean—a microcosm experiment. *Deep Sea Res II* 52:3011–3023
- Zubkov MV, Tarran GA (2008) High bacterivory by the smallest phytoplankton in the North Atlantic Ocean. *Nature* 455:224–227